The reagent vibrational excitation effect on the stereodynamics of the reaction $O(^1D) + HBr \rightarrow OH + Br$*

Zhang Ying-Ying(张莹莹)[a], Shi Ying(石 英)[a]†, Xie Ting-Xian(解廷献)[b], Jin Ming-Xing(金明星)[a], and Hu Zhan(胡 湛)[a]

[a] *Institute of Atomic and Molecular Physics, Jilin University, Changchun* 130012, *China*
[b] *Department of Physics, Dalian Jiaotong University, Dalian* 116028, *China*

(Received 10 December 2012; revised manuscript received 15 February 2013)

Calculations on the dynamics of the reaction $O(^1D) + HBr \rightarrow OH + Br$ are performed on the *ab initio* potential energy surfaces (PESs) of the ground state given by Peterson [Peterson K A *J. Chem. Phys.* **113** 4598 (2000)] using the quasi-classical trajectory (QCT) method. The product distribution of the dihedral angle, $P(\phi_r)$, and that of the angle between $\boldsymbol{k}$ and $\boldsymbol{j}'$, $P(\theta_r)$, are presented in three dimensions. Moreover, we also investigate the reagent vibrational excitation effects on the two polarization-dependent generalized differential cross sections (PDDCS), $PDDCS_{00}$ and $PDDCS_{20}$, in the center-of-mass frame. The results indicate that the vector properties are sensitive to the reagent vibrational quantum number.

Keywords: stereodynamics, quasi-classical trajectory, polarization-dependent generalized differential cross sections

PACS: 34.50.Lf, 82.20.Fd, 82.20.Kh **DOI:** 10.1088/1674-1056/22/8/083402

1. Introduction

Reactions of atomic oxygen with bromine-containing species play an important role in the chemistry of the upper atmosphere of the earth.[1–3] The reaction of $O(^1D) + HBr$ can be considered as a good prototype of the oxygen with brominated compounds. The title reactions take place on singlet potential surfaces with zero activation energy, while $O(^3P)$ reactions proceed on triplet surfaces with significant activation energies.[4] There are two competing pathways proceeding with considerable probability, that is,

$$O(^1D) + HBr \rightarrow \begin{cases} \rightarrow Br + OH, & \Delta H_0 = -60.0 \pm 1.0 \text{ kcal/mol}, \\ \rightarrow H + BrO, & \Delta H_0 = -13.9 \pm 1.4 \text{ kcal/mol}. \end{cases}$$

During the past 30 years, both experimental and theoretical studies have reported on the relevant chemical reactions. The characterizations of all the vibrational fundamentals of HOBr[5,6] as well as the pure rotational spectra and molecular dipole moment have been reported.[7] The yield of $H + BrO$ channel from the $O(^1D) + HBr$ reaction has also been reported in previous literature. Time-resolved resonance fluorescence detection has been employed by Wine *et al.*[8] Using the crossed molecular beam and infrared chemiluminescence methods, Balucani *et al.*[4] demonstrated that a lower limit to the branching ratio of the BrO + H/OH + Br which is derived from their experimental results. Meanwhile, in the molecular beam study they reported on a significant yield for the $H + BrO$ channel, and in the flash-photolysis study they reported on a very small yield. Given that the title reaction is fast, the BrO product of the title reaction has been detected by time-resolved ultraviolet (UV) absorption spectroscopy.[9]

In the theoretical respect, few studies have been performed to deal with the title reaction. One of the earliest studies can be traced to that of McGrath and Rowland, who calculated a value of formation heat and determined the equilibrium structure, harmonic frequencies, and relative energies of HOBr and its less stable isomer HBrO.[10] Peterson[11] constructed a new global *ab initio* potential energy surface, which was used to calculate the stereodynamics of the title reaction. Previous theoretical studies provided the impetus for the development of theoretical methods to simulate the measured profiles and to provide an insight into that information about the stereodynamics, which has not been obtained yet. Recently, using the time-dependent wave packet methods, Tang *et al.*[12] have computed the reaction probabilities and thermal rate constants, which are nearly independent of temperature.

With the rapid development of theoretical methods, many semiclassical and quantum theories have been developed in this stereodynamics field, and thus provided the necessary utilities to extract stereodynamical information. Very recently, quasi-classical trajectory (QCT) procedures have been developed by Wang *et al.*[13] and Chen *et al.*[14] with simultaneous treatment of propagating trajectories and obtaining the stereodynamical quantities, particularly those characterizing two- and three-vector correlations. Many studies on the heavy-light-heavy (HLH) systems, such as $O + HCl$,[15] $Sr + HF$,[16]

*Project supported by the Natural Science Fund from Jilin University, China (Grant No. 419080106440), the Chinese National Fusion Project for ITER (Grant No. 2010GB104003), and the National Natural Science Foundation of China (Grant No. 10974069).

†Corresponding author. E-mail: shi_ying@jlu.edu.cn

© 2013 Chinese Physical Society and IOP Publishing Ltd

and Ca + HCl[17] have been conducted. However, to the best of our knowledge, the reagent vibration excitation effects on the vector properties of the title deep-well reaction have not been studied yet. There exist difficulties in using either the traditional QCT method or the QM method to perform the vector correlation of the title reaction, because the deep potential well on the singlet potential energy surface and the heavy oxygen mass requires a large quantum basis set, leading to unaffordable CPU time and cost.[18] The problem can be solved using the newly developed QCT method in Refs. [13] and [14].

In this paper, we study the stereodynamics of the title reaction using a complete QCT method and obtain more information about the dynamics when directional properties are not explicitly considered. The influence of the reagent vibrational excitation of the hydrogen molecule on the vector correlation of the product is also discussed.

2. Computational methods

The ground-state potential energy surface (PES) obtained from *ab initio* data of Peterson *et al.*[11] is used in this work. Compared with other reactions, the title reaction has a deep well on the singlet PES which leads to a long-lifetime intermediate complex. Moreover, Tang *et al.*[12] have also proved that the *ab initio* calculations of HOBr are nearly identical to previous results of HOCl[19,20] and the stability and reliability of the calculated results below can be guaranteed[21,22] with high vibrational levels. The calculation method of QCT is similar to that described in Refs. [23]–[26]. In our calculations, the center-of-mass (CM) frame is employed as shown in Fig. 1. The z axis is parallel to the reagent initial relative velocity vector $\boldsymbol{k}$, and the y axis is perpendicular to the xz scattering plane which contains $\boldsymbol{k}$ and $\boldsymbol{k}'$. θ_r is the angle between $\boldsymbol{j}'$ and $\boldsymbol{k}$, and ϕ_r is the dihedral angle of the $\boldsymbol{k}$–$\boldsymbol{k}'$–$\boldsymbol{j}'$ correlation. They also refer to the polar angle and the azimuth angle of the vector $\boldsymbol{j}'$, respectively. All of these angles can be derived from the QCT dynamical calculations, where the Hamiltonian motion equations are numerically solved by an efficient six-order symplectic integration procedure in three dimensions.

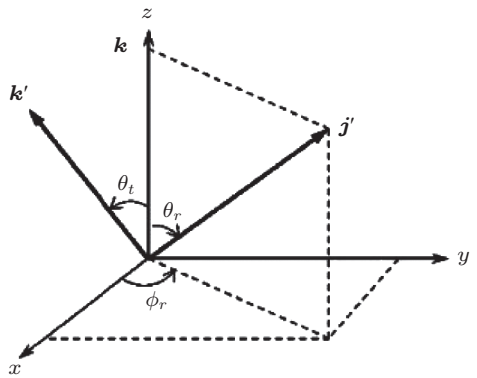


Fig. 1. The center-of-mass coordinate system used to describe the $\boldsymbol{k}, \boldsymbol{k}'$, and $\boldsymbol{j}'$ correlations.

The vibrational and rotational quantum numbers of reactant molecules in the present work are chosen to be $v = 0$–7 and $j = 0$, respectively. The initial trajectories are at O–HBr internuclear separations of 10 Å. In this work, the collision energy of the title reaction is chosen to be 0.3 eV and a set of 5×10^4 trajectories were run for each vibrational quantum number. The integration step size of 0.1 fs is used to ensure numerical stability. The accuracy of the numerical integration is verified by checking the conservation of the total energy and total angular momentum for each trajectory. The average rotational alignment parameter $\langle P_2(j' \cdot k)\rangle$ is also calculated in our work.

The functions of $P(\theta_r)$, $P(\phi_r)$, and $P(\theta_r, \phi_r)$ are expanded as follows:[27–33]

$$P(\theta_r) = \frac{1}{2}\sum_k [k] a_0^k P_k(\cos\theta_r), \tag{1}$$

where $a_0^k = \langle P_k(\cos\theta_r)\rangle$, and $[k] = 2k+1$.

$$P(\phi_r) = \frac{1}{2\pi}\left(1 + \sum_{n_{\text{even}}\geq 2} a_n \cos n\phi_r + \sum_{n_{\text{odd}}\geq 1} b_n \sin n\phi_r\right), \tag{2}$$

where the expansion coefficients are given by

$$a_n = 2\langle \cos n\phi_r\rangle, \quad b_n = 2\langle \sin n\phi_r\rangle, \tag{3}$$

$$\begin{aligned} P(\theta_r, \phi_r) &= \frac{1}{4\pi}\sum_{kq} [k]\, a_q^k C_{kq}(\theta_r, \phi_r)^* \\ &= \frac{1}{4\pi}\sum_k \sum_{q\geq 0} [a_{a\pm}^k \cos q\phi_r \\ &\quad - a_{q\mp}^k i \sin q\phi_r] C_{kq}(\theta_r, 0), \end{aligned} \tag{4}$$

where

$$a_0^k = \begin{cases} 2\langle C_{K|q|}(\theta_r, 0)\cos q\phi_r\rangle, & (k = \text{even}), \\ 2\langle C_{K|q|}(\theta_r, 0)\sin q\phi_r\rangle, & (k = \text{odd}), \end{cases}$$

$$\frac{1}{\sigma}\frac{\mathrm{d}\sigma_{kq\pm}}{\mathrm{d}\omega_t} = \sum_{k1}\frac{[k_1]}{4\pi} S_{kq\pm}^{k1} C_{k1-q}(\theta_{\mathrm{T}}, 0), \tag{5}$$

$$S_{kq\pm}^{k1} = \langle c_{k1q}(\theta_t, 0) c_{kq}(\theta_r, 0)[(-1)^q \mathrm{e}^{\mathrm{i}q\phi_r} \pm \mathrm{e}^{-\mathrm{i}q\phi_r}]\rangle. \tag{6}$$

Here, $(1/\sigma)(\mathrm{d}\sigma_{kq\pm}/\mathrm{d}\omega_t)$ is the polarization-dependent generalized differential cross section (PDDCS), and the angular brackets represent an average over all the reactive trajectories. The corresponding details of the above equations are available in Ref. [13].

3. Results and discussion

In order to see the vector correlation functions and the PDDCS directly, we plot them in three dimensions. Figure 2 illustrates the calculated product distribution of $P(\theta_r)$ on different vibrational levels of the $O(^1D) + HBr$ reaction. The distribution of $P(\theta_r)$ representing the $\boldsymbol{k}$–$\boldsymbol{j}'$ correlation indicates

that the rotational alignment of the product is very strong. For different vibrational quantum numbers, the peaks of $P(\theta_r)$ are located at $\theta_r = 90^\circ$ and symmetric with respect to the direction of 90° because of the planar symmetry of the system. This implies that the product rotational angular momentum vector $\boldsymbol{j}'$ is strongly aligned along the direction perpendicular to the relative velocity direction. Moreover, the peaks of $P(\theta_r)$ become higher and narrower as the vibrational quantum number increases, indicating that the product alignment becomes stronger at high vibrational levels.

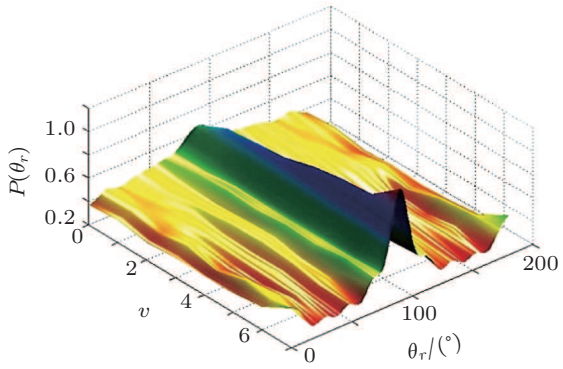


Fig. 2. (color online) Distributions of $P(\theta_r)$ reflecting $\boldsymbol{k}$–$\boldsymbol{j}'$ correlations at different vibrational levels $v = 0$–7 for the reagent rotational excitation.

The dihedral angle distributions $P(\phi_r)$ describing the correlation of $\boldsymbol{k}$–$\boldsymbol{k}'$–$\boldsymbol{j}'$ are plotted in Fig. 3. The vibrational quantum number from inside to outside changes from $v = 0$ to $v = 7$, and ϕ_r increases in the clockwise direction. The calculated results of $P(\phi_r)$ are in good agreement with the results obtained by Wang *et al.*[34] that the distribution of $\boldsymbol{j}'$ does not have azimuthal symmetry for the H + LH mass combination (H: heavy, L: light) on the repulsive potential energy surface. We can see that the distributions of $P(\phi_r)$ tend to be asymmetric with respect to the scattering plane, directly reflecting the strong polarization of the angular momentum induced by the PES. There are two sharp peaks at $\phi_r = 90^\circ$ and $\phi_r = 270^\circ$ in all vibrational quantum numbers, which means that the product rotational angular momentum vector $\boldsymbol{j}'$ is aligned along the y axis in the CM frame. The peaks at $\phi_r = 90^\circ$ are stronger than those at $\phi_r = 270^\circ$, indicating that $\boldsymbol{j}'$ is oriented along the positive direction of the y axis.

The asymmetry of $P(\phi_r)$ can be described qualitatively by an impulse model. Based on the previous studies,[35,36] it results, most likely, from the repulsive energy between H–Br atoms, which leads to the violation of the symmetry when the reaction occurs. The product angular momentum vector $\boldsymbol{j}'$ can be written as

$$j' = L\sin^2\beta + j\cos^2\beta + J_1 m_A/m_B, \quad (7)$$

$$J_1 = (\mu_{BC}R)^{1/2}(\boldsymbol{r}_{AB} \times \boldsymbol{r}_{CB}). \quad (8)$$

Here, L is the reagent orbital angular momentum, μ_{BC} the reduced mass of the BC molecule, R is the repulsive energy, $\boldsymbol{r}_{AB}$ and $\boldsymbol{r}_{CB}$ are the unit vectors with B pointing to A and C, respectively, and $\cos^2\beta$ is the mass factor. In the reaction $O(^1D) + HBr$, the term $L\sin^2\beta + j\cos^2\beta$ is symmetric, while the term $J_1 m_A/m_B$ shows a preferential direction for the effect of repulsive energy, leading to the left-handed product rotation in plane parallel to the scattering plane.[22] The distribution of $P(\phi_r)$ which is strongly affected by the vibrational quantum numbers can be attributed to the fact that the O atom has relatively strong absorbability to charges. At higher vibrational levels, the O atom can rapidly and easily capture the H atom from the HBr molecule. Therefore, the product molecular rotational angular momentum vector $\boldsymbol{j}'$ tends to be weakly aligned and oriented along the y axis with the increase of vibrational quantum number.[37–44]

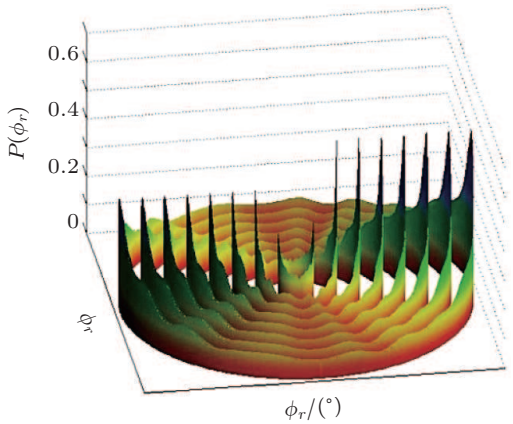


Fig. 3. (color online) Dihedral angle distribution of $P(\phi_r)$ with respect to the $\boldsymbol{k}$–$\boldsymbol{k}'$ plane, plotted at reagent vibrational quantum numbers from inside to outside are $v = 0$ to $v = 7$, respectively.

In order to further support the above-mentioned findings associated with the influence of the vibrational quantum number, the distributions of $P(\theta_r, \phi_r)$ averaged over all the scattering angles are plotted. For simplicity and without loss of generality, we show in Fig. 4 only the joint $P(\theta_r, \phi_r)$ distributions with peaks and valleys at three vibrational levels: $v = 0$, 3, 6. In Fig. 4, the distributions of $P(\theta_r, \phi_r)$ with peaks at $(90^\circ, 90^\circ)$ and $(90^\circ, 270^\circ)$ are in accordance with the distributions of $P(\theta_r)$ and $P(\phi_r)$ of OH products for all vibrational quantum numbers, although there are some shape differences. The distribution of $P(\theta_r, \phi_r)$ indicates that the OH products are preferentially polarized in the direction perpendicular to the scattering plane, and mainly rotate in the plane parallel to the scattering plane.[45–52]

The QCT PDDCSs are used to describe the $\boldsymbol{k}$–$\boldsymbol{k}'$–$\boldsymbol{j}'$ correlation and the scattering direction of the OH product molecule. In the present work, the $PDDCS_{00}$ $(2\pi/\sigma)(d\sigma_{00}/d\omega_t)$ and $PDDCS_{20}$ $(2\pi/\sigma)(d\sigma_{20}/d\omega_t)$ are calculated. Figure 5(a) shows the calculated $PDDCS_{00}$ as a function of the scattering angle θ_T for the vibrational quantum number ranging from $v = 0$ to $v = 7$. The $PDDCS_{00}$ is a simple differential cross section which only describes the $\boldsymbol{k}$–$\boldsymbol{k}'$ correlation or the scattering direction of the product, and is

not associated with the orientation and alignment of the product rotational angular momentum vector $\boldsymbol{j}'$. Specifically, it can be seen that at different vibrational quantum numbers, the product OH is largely scattered forward at the scattering angle θ_T ranging from 0° to 45°, and weakly scattered backward in an angle range of 140°–180°. We can also conclude that with the increase of vibrational quantum number, the product forward scattering becomes stronger, and the backward scattering becomes weaker and tends to convert into sideward scattering.

The $PDDCS_{20}$ is the expectation value of the second Legendre moment $\langle P_2(j'\cdot z)\rangle$ as shown in Fig. 5(b). The values of $PDDCS_{20}$ are almost negative in the whole scope. This may be ascribed to the fact that the $PDDCS_{20}$ correlates with the alignment moment $\langle P_2(j'\cdot k)\rangle$, which is listed in Table 1. We can see its trend opposite to that of $PDDCS_{00}$ over the range of the scattering angles, which means that $\boldsymbol{j}'$ is strongly aligned along the direction perpendicular to $\boldsymbol{k}$. It is also obvious that the alignment of the product becomes stronger with the increase of vibrational quantum number.

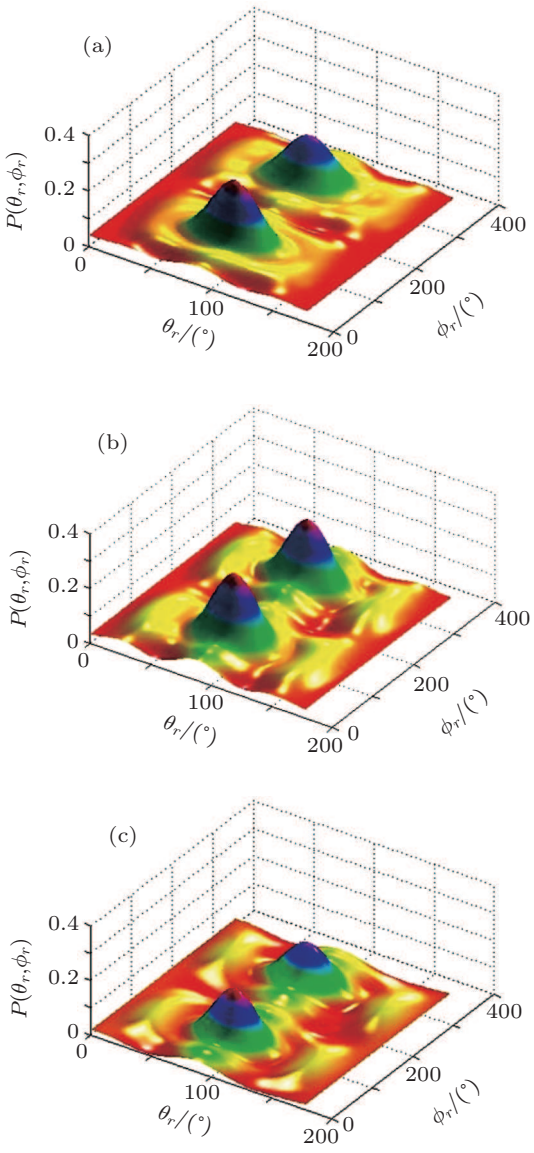


Fig. 4. (color online) Polar plots of the $P(\theta_r,\phi_r)$ distributions with peaks and valleys at different vibrational levels: (a) $v=0$; (b) $v=3$; (c) $v=6$.

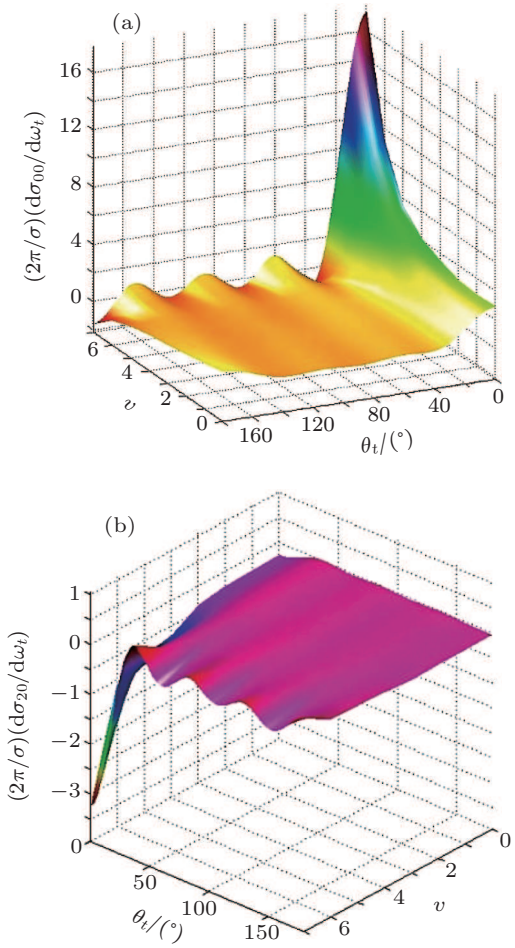


Fig. 5. (color online) Two PDDCSs of the reagent vibrational quantum numbers with (a) $(k,q)=(0,0)$; (b) $(k,q)=(2,0)$, respectively.

Table 1. Variation of rotational alignment parameter $\langle P_2(j'\cdot k)\rangle$ with vibrational levels $v=0$ to $v=7$ for the title reaction.

Vibration level	$v=0$	$v=1$	$v=2$	$v=3$	$v=4$	$v=5$	$v=6$	$v=7$
$\langle P_2(j',k)\rangle$	–0.36793	–0.37516	–0.37626	–0.3749	–0.39131	–0.39459	–0.39543	–0.41659

4. Conclusions

The QCT method has been used in our work to study the dynamics and the reagent vibrational excitation effect on the stereodynamics of the title reaction in the ground state of *ab initio* potential energy surfaces (PESs) at vibrational levels from $v=0$ to $v=7$. The distributions of $P(\theta_r)$ and $P(\phi_r)$ of the products for the title reactions are calculated. The $P(\theta_r)$

distribution suggests that $\boldsymbol{j}'$ is strongly aligned along the direction perpendicular to $\boldsymbol{k}$ and the distribution $P(\phi_r)$ shows that the product rotational angular momentum vector $\boldsymbol{j}'$ is oriented along the positive direction of the y axis of the CM frame, it can be well explained by impulse model. In addition, we have calculated two PDDCSs: PDDCS_{00} and PDDCS_{20}. The PDDCS_{00} demonstrates that with the increase of vibrational quantum number, the OH product is strongly scattered forward and weakly scattered backward, and has a trend of turning into sideward scattering. The PDDCS_{20} indicates that $\boldsymbol{j}'$ is strongly aligned in the direction perpendicular to $\boldsymbol{k}$. In summary, the calculated results clearly indicate that vector properties are sensitive to the reagent vibrational quantum number.

Acknowledgment

Many thanks to Prof. Han Ke-Li for providing the stereodynamics program.

References

[1] Yagi K, Williams J, Wang N Y and Cicerone R J 1995 *Science* **267** 1979
[2] Tie X X and Brasseur G 1996 *Geophys. Res. Lett.* **23** 2505
[3] Mahmud K, Kim J S and Fontijn A 1990 *J. Phys. Chem.* **94** 2994
[4] Balucani N, Beneventi L, Casavecchia P, Volpi G G, Kruss E J and Sloan J J 1994 *Can. J. Chem.* **72** 888
[5] McRae G A and Cohen E A 1990 *J. Mol. Spectrosc.* **139** 369
[6] Koga Y, Takeo H, Kondo S, Sugie M, Matsumura C, McRae G A and Cohen E A 1989 *J. Mol. Spectrosc.* **138** 467
[7] Cohen E A, McRae G A, Tan T L, Friedl R R, Johns J W C and Noel M 1995 *J. Mol. Spectrosc.* **173** 55
[8] Wine P H, Wells J R and Ravishankara A R 1986 *J. Chem. Phys.* **84** 1349
[9] Cronkhite J M and Wine P H 1998 *Int. J. Chem. Kinet.* **30** 555
[10] McGrath M P and Rowland F S 1994 *J. Phys. Chem.* **98** 4774
[11] Peterson K A 2000 *J. Chem. Phys.* **113** 4598
[12] Tang B Y, Tang Q K, Chen M D, Han K L and Zhang J Z H 2004 *J. Chem. Phys.* **120** 8537
[13] Wang M L, Han K L, Zhan J P, Wu V W K, He G Z and Lou N Q 1997 *Chem. Phys. Lett.* **278** 307
[14] Chen M D, Han K L and Lou N Q 2002 *Chem. Phys.* **283** 463
[15] Zhu T, Hu G D, Chen J Z, Liu X G and Zhang Q G 2010 *Chin. Phys. B* **19** 083402
[16] Cai M Q, Zhang L, Tang B Y, Chen M D, Yang G W and Han K L 2000 *Chem. Phys.* **260** 281
[17] Tang P Y, Li D L, Wu M M and Tang B Y 2011 *J. Theor. Comput. Chem.* **10** 19
[18] Chu T S, Zhang Y and Han K L 2006 *Int. Rev. Phys. Chem.* **25** 201
[19] KoKov S S, Peterson K A and Bowman J M 1998 *J. Chem. Phys.* **109** 2662
[20] Peterson K A, KoKov S S and Bowman J M 1999 *J. Chem. Phys.* **111** 7446
[21] Pijkeren D V, Eck J V and Niehaus A 1983 *Chem. Phys. Lett.* **96** 20
[22] Chen M D, Han K L and Lou N Q 2002 *Chem. Phys. Lett.* **357** 483
[23] Sizun M, Song J B and Gislason E A 2002 *J. Chem. Phys.* **116** 2888
[24] De Miranda M P, Aoiz F J, Brouard M and Saez-Rabanos V 2004 *J. Chem. Phys.* **121** 9830
[25] De Miranda M P and Clary D C 1997 *J. Chem. Phys.* **106** 4509
[26] Zhao J, Xu Y and Meng Q T 2010 *Chin. Phys. B* **19** 063403
[27] Chen M D, Han K L and Lou N Q 2003 *J. Chem. Phys.* **118** 4463
[28] Xu W W, Liu X G, Luan S X, Sun S S and Zhang Q G 2009 *Chin. Phys. B* **18** 339
[29] Wang M L, Han K L and He G Z 1998 *J. Chem. Phys.* **109** 4463
[30] Han K L, Zhang L, Xu D L, He G Z and Lou N Q 2001 *J. Phys. Chem. A* **105** 2956
[31] Zhang W Q, Li Y Z, Xu X S and Chen M D 2010 *Chem. Phys.* **367** 115
[32] Liu Y F, Zhang W, Shi D H and Sun J F 2009 *Chin. Phys. B* **18** 4264
[33] Li H, Zheng B and Meng Q T 2012 *Acta Phys. Sin.* **61** 153401 (in Chinese)
[34] Wang M L, Han K L and He G Z 1998 *J. Phys. Chem. A* **102** 10204
[35] Yao L, Zhong H Y, Liu Y L and Xia W W 2009 *Chem. Phys.* **359** 151
[36] Liu S L and Shi Y 2011 *Chem. Phys. Lett.* **501** 197
[37] Li H, Zheng B, Yin J Q and Meng Q T 2011 *Chin. Phys. B* **20** 123401
[38] Zhang W Q, Cong S L, Zhang C H, Xu X S and Chen M D 2009 *J. Phys. Chem.* **113** 4192
[39] Gómez-Carrasco S, González-Sánchez L and Aguado A 2004 *Chem. Phys. Lett.* **383** 25
[40] Zhao L, Sun P and Liu C Z 2011 *Chin. Phys. Lett.* **28** 083101
[41] Liu Y F, He X H, Shi D H and Sun J F 2011 *Chin. Phys. B* **20** 078201
[42] Aldegunde J, Aoiz F J and Gonzalez-Sanchez L 2012 *Phys. Chem. Chem. Phys.* **14** 2911
[43] Fu Y B, Luo W L, Ruan W, Zhang L and Zhu Z H 2009 *Chin. Phys. B* **18** 167
[44] Liu S L and Shi Y 2010 *Chem. Phys. Lett.* **27** 123103
[45] Han K L, Zheng X G, Sun B F, He G Z and Zhang R Q 1991 *Chem. Phys. Lett.* **181** 474
[46] Hartree W S and Simons J P 1990 *J. Chem. Soc. Faraday Trans.* **86** 17
[47] Liu S L and Shi Y 2011 *Chin. Phys. B* **20** 013404
[48] Han K L, Zheng X G, Sun B F and He G Z 1991 *Chem. Phys. Lett.* **181** 47
[49] Xu Y, Zhao J, Yue D G, Liu H, Zheng X Y and Meng Q T 2009 *Chin. Phys. B* **18** 5308
[50] Cheng J and Yue X F 2011 *Chin. Phys. Lett.* **28** 083102
[51] Zheng Y J and Ge M H 2011 *Chin. Phys. B* **20** 083401
[52] Zhao J and Luo Y 2011 *Chin. Phys. B* **20** 083402